Journal of Organometallic Chemistry, 472 (1994) 149–162

Synthesis and chemistry of heterobimetallic fulvalene complexes containing W, Mo, and Rh *

Andrew P. Kahn [1], Roland Boese [2], Janet Blümel [3,*] and K. Peter C. Vollhardt *

Department of Chemistry, University of California at Berkeley, Berkeley, CA 94720 (USA)

(Received January 7, 1994; in revised form February 11, 1994)

Abstract

The photo- and thermal chemistry of the heterobimetallic fulvalene (Fv) complex Fv[$W(CO)_3Me$][$Rh(CO)_2$] (**1**) was investigated, and compounds $Fv(CO)_2MeWRh(CO)[\mu\text{-}CO]$ (**2**), $Fv(CO)_3WRh(CO)Me$ (**3**), and $Fv(CO)_3WRh(CO)C(O)Me$ (**4**) were characterized. Reaction mechanisms were studied by labeling experiments using ^{13}CO and by analogy to the Mo–Rh system. The complexes $Fv(CO)_3MoRh(CO)C(O)Me$ (**7**) and $Fv(CO)_3MoRh(CO)Me$ (**8**) were characterized. Reaction of **3** and **4** with PMe_3 gave the zwitterionic species Fv[$W(CO)_3$][$Rh(PMe_3)_2Me$] (**16**) and Fv[$W(CO)_3$][$Rh(PMe_3)_2C(O)Me$] (**17**), respectively. An excess of PMe_3 led to the mononuclear compounds $FvRh(PMe_3)_2Me$ (**18**) and $FvRh(PMe_3)_2C(O)Me$ (**19**). The latter was reacted with $Mo(CO)_3(EtCN)_3$ to give zwitterionic Fv[$Mo(CO)_3$][$Rh(PMe_3)_2C(O)Me$] (**20**). The X-ray structures of the acyl complexes **4** and **17** were obtained. X-ray data of **4**: $P\bar{1}$, $a = 13.529(3)$ Å, $b = 15.813(3)$ Å, $c = 16.164(3)$ Å, $\alpha = 62.72(1)°$, $\beta = 87.24(1)°$, $\gamma = 86.32(1)°$, $V = 3065.9(11)$ Å^3, $Z = 8$, $R_w = 0.045$. X-ray data of **17**: $P2_1/n$, $a = 15.412(4)$ Å, $b = 9.745(2)$ Å, $c = 18.209(6)$ Å, $\alpha = 90.0°$, $\beta = 93.46(2)°$, $\gamma = 90.0°$, $V = 2730.0(22)$ Å^3, $Z = 4$, $R_w = 0.0303$.

Key words: Tungsten; Molybdenum; Rhodium; Heterobimetallics; Fulvalene

1. Introduction

The chemistry of fulvalene-bridged analogs of Cp–metal dimers has been the focus of significant recent attention [1,2]. Besides their interesting electrochemical [3] and magnetic [4] properties, the reactivities of fulvalene (Fv) complexes should differ from that of their Cp analogs, because of the possibility of electronic communication between the metal nuclei through the π system of the ligand [3] or lengthening and thus weakening of eventual metal–metal bonds by the steric requirements of the Fv ligand [1]. Additionally, combining the properties of two different metals should give rise to unique reactivity features, especially compared to those found in homobimetallic systems. Thus, for example, the heterodinuclear complex $Fv(CO)_2Ru$-$Mo(CO)_3$ differed in reactivity from the corresponding homodinuclear fulvalene complexes [2].

We have recently developed an efficient site-specific synthesis for heterodinuclear fulvalene complexes and prepared various tungsten-containing species [5]. Here we report on the thermal and photochemistry of Fv[$W(CO)_3Me$][$Rh(CO)_2$] (**1**) and $Fv(CO)_2MeWRh(CO)[\mu\text{-}CO]$ (**2**). The W, Rh system is of special interest, because both its Cp analogs, $CpW(CO)_3Me$ [6–8] and $CpRh(CO)_2$ [9–12] are already well explored. The behavior of this Cp compounds suggests that **1** might undergo dimerization upon irradiation, with formation of a metal–metal bond. This was also observed for the homobimetallic complex Fv[$W(CO)_3Me$]$_2$, which gave $Fv(CO)_3WW(CO)_3$ with accompanied C–H activation in the solvent benzene [13]. C–H activation is also possible at the Rh center of **1**, since $CpRh(CO)_2$, embedded in a methane matrix, yielded $CpRhH(CO)$-Me upon irradiation [10]. In solution, C–H activation of cyclohexane was observed [11]. With respect to C–H

Correspondence to: Professor K.P.C. Vollhardt or Dr. J. Blümel.

* Dedicated to Prof. Dr. Helmut Werner on the occasion of his 60th birthday.

[1] Present address: ARCO Chemicals, New Town Square, PA 19073, USA.

[2] Present address: Institut für Anorg. Chemie, Universität-GH Essen, Universitätsstr. 5–7, 45117 Essen, Germany.

[3] Present address: Anorg.-chem. Institut der TU München, Lichtenbergstr. 4, 85747 Garching, Germany.

0022-328X/94/$7.00
SSDI 0022-328X(94)24595-A

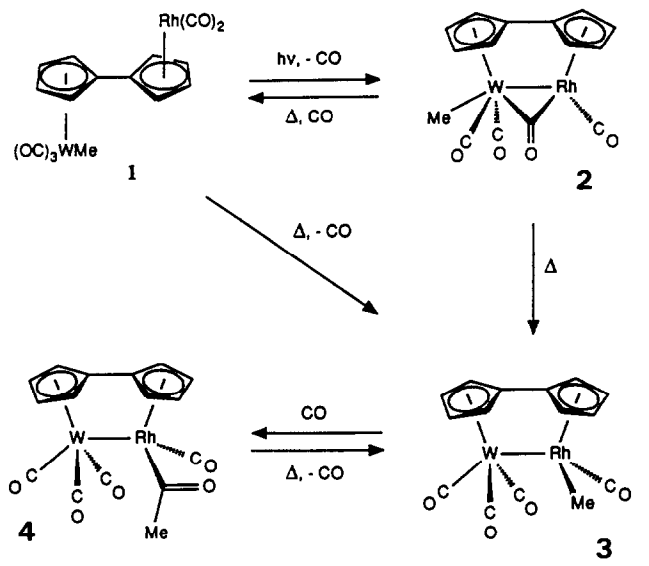

Scheme 1. Photo- and thermal chemistry of fulvalene complexes 1–4.

activation, heterobimetallic **1** seems especially attractive, because the methyl group is located in close proximity to the Rh center. This constitutes an ideal prerequisite for insertion of Rh into a C–H bond of the neighboring methyl group, resulting perhaps in a structure like $Fv(CO)_3WRhHCO[\mu\text{-}CH_2]$. In addition to that, the identification of compounds containing the spin-1/2 nuclei ^{183}W and ^{103}Rh (14% and 100% natural abundance) by NMR spectroscopy should be facilitated by the observation of characteristic *J*-coupling values.

2. Results and discussion

2.1. Photochemistry of $Fv[W(CO)_3Me][Rh(CO)_2]$

$Fv[W(CO)_3Me][Rh(CO)_2]$ (**1**) was synthesized in about 73% yield according to the procedure given in [5]. The UV-VIS spectrum of **1** with its absorption at $\lambda_{max} = 301$ nm suggested that **1** should be photosensitive to light of this wavelength. Indeed, irradiation of a THF solution of **1** led to the loss of one CO ligand and gave **2**, a metal–metal bonded fulvalene complex with one bridging CO ligand (Scheme 1) in 55% yield.

The presence of a bridging carbonyl group was indicated by the absorption at 1775 cm^{-1} [14,15], distinct from those of the terminal counterparts of 2008, 1967, and 1905 cm^{-1}. All the other spectral and analytical data were consistent with the proposed formulation of **2**.

2.2. Fluxional behavior of $Fv(CO)_2MeWRh(CO)[\mu\text{-}CO]$ (2)

Measuring the proton NMR spectrum of **2** at −60°C gave the eight expected fulvalene multiplets, located between 6.4 and 4.4 ppm. The protons of the methyl group resonated at 0.35 ppm. The acquisition of the ^{13}C NMR spectrum at this temperature revealed the presence of two carbonyl ligands associated with the rhodium center. Both signals gave rise to doublets, centered at 246.89 and 194.54 ppm, respectively. The former exhibited a $J(^{103}Rh-^{13}C)$ value of 37 Hz, consistent with a bridging interaction, while the latter was split by 93 Hz, a value commonly observed for CO terminally bound to rhodium [14,15]. In addition, the methyl carbon resonated as a singlet positioned at −18.84 ppm, consistent with the assignment of this group to the tungsten nucleus. The W–CO signals (219.32 and 209.98 ppm) and the 10 fulvalene peaks (located between 111 and 83 ppm) were in accord with the absence of symmetry in the complex.

On warming to room temperature, the ^1H NMR spectrum became quite featureless, exhibiting only a sharp singlet at 0.38 ppm (3 H), that was assigned to the protons of the tungsten-bound methyl group, and a broad single peak at 5.92 ppm (2 H). Unfortunately, the molecule thermally rearranged at temperatures above 90°C. Nevertheless, as the temperature of the sample was elevated, fulvalene multiplets began to emerge in the ^1H NMR spectrum at 5.86 ppm ("t", $J = 2.4$ Hz, 2 H), corresponding probably to the signal at 5.92 ppm of the room temperature measurement, 5.38 ppm (br s, 4 H), and 5.16 ppm (br s, 2 H), while the ^1H NMR signal of the methyl group remained unchanged.

The temperature dependence of the spectra suggests a fluxional process. Since the shape and position of the ^1H methyl resonance does not change with temperature, while all the fulvalene ^1H signals do, the most probable fluxional process is bridged-terminal carbonyl interchange involving only the rhodium COs (Scheme 2).

This parallels the fluxional behavior studied for $CH_2[(\eta^5\text{-}C_5H_4)M(CO)]_2(\mu CO)$, where M = Rh and Ir [14]. At the fast exchange limit of this type of motion, the alkyl ligand is maintained in one magnetic environment while a plane of symmetry parallel to the metal–metal bond is created.

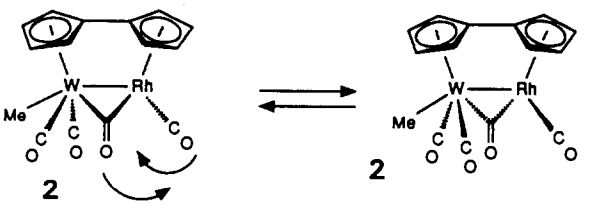

Scheme 2. Fluxional process of **2**.

2.3. Thermal chemistry of $Fv[W(CO)_3Me][Rh(CO)_2]$ (1) and $Fv(CO)_2MeWRh(CO)[\mu\text{-}CO]$ (2)

The photoreaction illustrated in Scheme 1 was thermally reversible, as shown by warming a THF solution of **2** under 1 atm of CO to regenerate **1**. In contrast, heating a toluene solution of **2** to reflux in the absence of added CO resulted in a color change from orange to red. Chromatography of the residue afforded the new product **3**, isolated as red crystals in 60% yield (Scheme 1). The spectral data clearly indicated that the methyl group had transferred from the tungsten center to the rhodium site. For example, in addition to the expected eight fulvalene multiplets (located between 6.2 and 4.3 ppm), the ^{1}H NMR spectrum exhibited a doublet centered at 0.68 ppm with a ^{103}Rh–^{1}H coupling constant of 2.5 Hz. Furthermore, the methyl carbon resonated in the ^{13}C NMR spectrum at −20.62 ppm, appearing as a doublet with $J(^{103}\text{Rh}-^{13}\text{C}) = 24.4$ Hz [15], while the signal for the CO ligand attached to rhodium could be found at 198.20 ppm, split by 83.0 Hz. This spectrum was acquired at −60°C to facilitate the observation of the W–CO resonances (225.02, 211.98, and 211.84 ppm).

Decarbonylative methyl group transfer from the W to the Rh center in **1** could also be promoted efficiently by direct thermolysis. Heating a toluene solution of **1** to reflux for 24 h resulted in a 70% yield of **3** (Scheme 1). When a THF solution of **3** was exposed to 1 atm. of CO at 45°C, smooth conversion to the rhodium acyl **4** took place, which could be isolated in 89% yield. The reversibility of this reaction was demonstrated by heating a toluene solution of **4** to reflux for six hours, resulting in an 84% recovery of **3** after recrystallization (Scheme 1).

The presence of the acyl group in **4** was readily confirmed through the use of NMR and IR spectroscopy. For example, in addition to the terminal carbonyl absorptions at 2011, 1965, 1905, and 1879 cm^{-1}, the IR spectrum (KBr) revealed a band at 1635 cm^{-1}, characteristic of an η^1-acyl complex [16]. The ^{1}H NMR spectrum exhibited the expected eight fulvalene multiplets (located between 6.2 and 4.0 ppm) as well as the signal for the acyl–methyl group at 2.51 ppm, in the range generally observed for other rhodium–acetyl functionalities [16]. Furthermore, the ^{13}C NMR spectrum exhibited a doublet for the acyl carbon centered at 225.92 ppm with a ^{103}Rh–^{13}C coupling constant of 30.8 Hz. The methyl carbon and terminal CO ligand also experienced coupling to the ^{103}Rh nucleus, resonating as doublets centered at 50.47 ($J(^{103}\text{Rh}-^{13}\text{C}) =$ 4.3 Hz) and 196.70 ($J(^{103}\text{Rh}-^{13}\text{C}) = 92.3$ Hz) ppm, respectively. The W–CO signals (223.88, 213.85, and 211.48 ppm) were slightly broadened, indicating the beginning of a dynamic process.

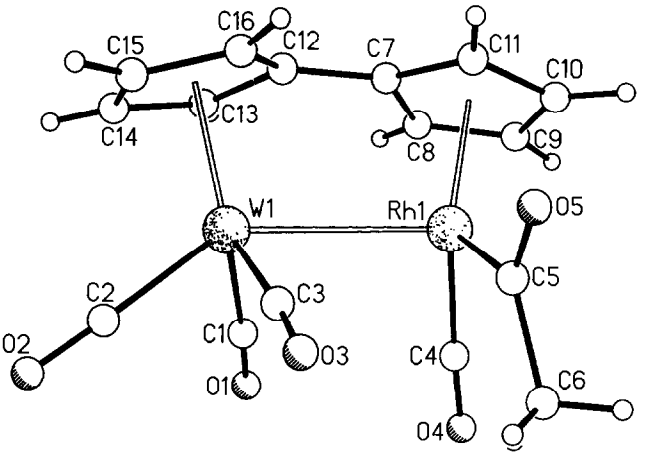

Fig. 1. SHELXTL drawing of $Fv(CO)_3WRh(CO)C(O)Me$ (**4**). Bond length and angle data are given in the text and in the supplementary material.

Crystals of **4**, suitable for an X-ray diffraction study, were obtained by slow diffusion of hexanes into a THF solution of **4**. A SHELXTL drawing of one of the four independent molecules found in the unit cell is shown in Fig. 1 and bond lengths and angle data are available with the supplementary material. The W–Rh bond length of 2.990(1) Å is the longest such structurally determined separation of its kind yet known, exceeding that of a model compound given in [17] by 0.23 Å. The length of this bond may be a consequence of the eclipsing interactions of the ligands on each metal inhibiting a closer metal–metal contact. Consistent with this notion is the greater distortion from linearity of the M–C–O angle for carbonyls 1, 3, and 4 (175.8(11)°, 173.9(11)°and 174.1(9)°, respectively) compared to carbonyl 2 (178.4(12)°). The dihedral angle between the planes created by the two Cp rings of the fulvalene ligand is 24.4° with a slight twist of 6.5°.

2.4. The chemistry of Mo–Rh–fulvalene complexes

The chemical [18] and electrochemical [19] properties of homodinuclear molybdenum fulvalene complexes have been the focus of recent research. Unique reactivity features were also found for the heterobimetallic fulvalene complex $Fv(CO)_2RuMo(CO)_3$ [2]. In addition, Cp molybdenum compounds are well explored and they are more reactive than their tungsten analogs [20]. Hence, the chemistry of Mo, Rh fulvalene compounds in comparison with the W, Rh analogs was of interest with respect to the possibility of fine tuning the reactivity of heterobimetallic Fv complexes.

In an attempt to prepare **6** from the diene **5** according to the procedure given in [5] at room temperature, instead of **6**, the acyl complex **7** was obtained directly as brown crystals after chromatography in about 60%

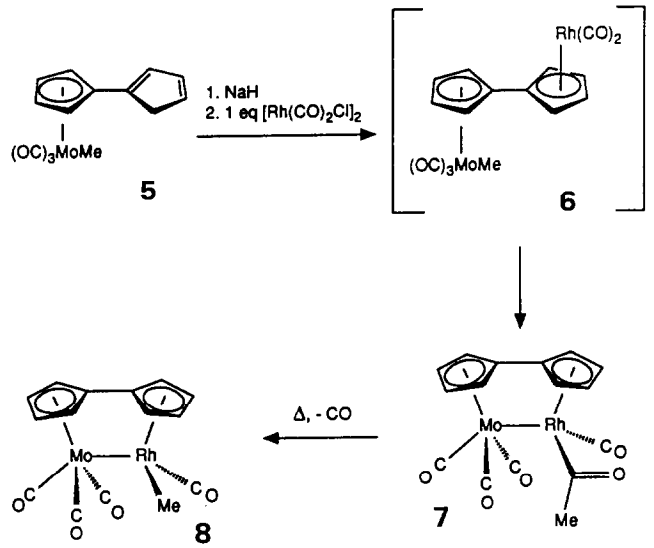

Scheme 3. Synthesis and thermal chemistry of acyl 7. The intermediate 6 was not observed.

yield (Scheme 3). All the analytical and spectral features of 7 were completely analogous to the ones observed for the tungsten acyl 4. Refluxing a toluene solution of 7 for about 2 h converted 7 to 8 quantitatively as judged by NMR spectroscopy. 8 gave brick red crystals when hexanes were allowed to diffuse slowly into a THF solution. The analytical and spectral characteristics of 8 were in accord with the formulation given in Scheme 3 and comparable to the ones of the corresponding tungsten compound 3.

2.5. Mechanistic studies including labeling experiments

In order to support the mechanisms for the reactions already outlined in Schemes 1 and 3, the fate of ^{13}CO in the corresponding labeled compounds was followed. In this effort, the labeled starting material **1-(^{13}C)$_2$** played a key role (Scheme 4).

2.5.1. Synthesis and characterization of 1-(^{13}C)$_2$

When a THF solution of 2 was warmed to 45°C for 17 h under 50 psi of ^{13}CO, **1-(^{13}C)$_2$** could be recovered as the only product (Scheme 4). ^{13}C NMR revealed a doublet centered at 192.16 ppm ($J(^{103}Rh-^{13}C) = 84.2$ Hz), the intensity of which confirmed that the label had incorporated into the Rh center only. Moreover,

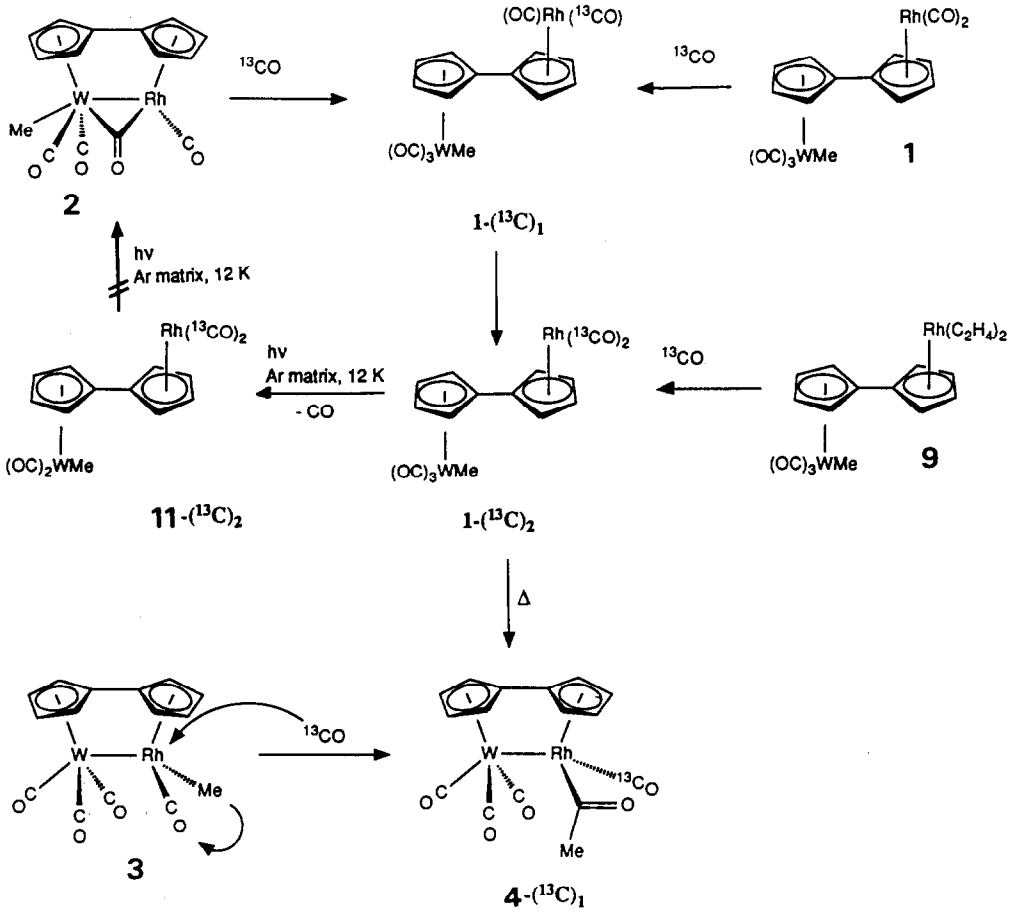

Scheme 4. ^{13}C labeling experiments to investigate the mechanisms of the reactions presented in Scheme 1.

the IR spectrum displayed four bands associated with carbonyl stretches at 2014, 2001, 1945, and 1933 cm^{-1}, corroborating, when compared with model compounds, the assumption, that both of the Rh–COs had been exchanged.

Additional confirmation of the double incorporation of the label could be obtained by mass spectral analysis, the spectrum of **1-(^{13}C)$_2$** exhibiting a broad peak envelope for the molecular ion that was shifted to mass units higher than that for **1**.

While the singly labeled derivative **1-(^{13}C)$_1$** was not actually detected during the conversion of **2** to **1-(^{13}C)$_2$**, the studies conducted by Basolo and co-workers [9] on the ligand substitution chemistry of $CpRh(CO)_2$ suggested that such a species most likely played an active role in the transformation.

Another synthesis of **1-(^{13}C)$_2$** is based on the assumption that **1** should be susceptible to ligand exchange reactions under similar conditions. Indeed, after 4 days at room temperature, **1**, dissolved in THF under 50 psi of ^{13}CO, had been entirely converted to **1-(^{13}C)$_2$** (Scheme 4). The IR spectrum of an aliquot of this reaction mixture taken after only one day displayed, in addition to the carbonyl stretching absorption for **1-(^{13}C)$_2$**, bands at 2032, 2015, 1961, and 1934 cm^{-1} attributed to the monolabeled product Fv[W(CO)$_3$Me][Rh(CO)(^{13}CO)] (**1-(^{13}C)$_1$**).

From a preparative standpoint, the most convenient route to **1-(^{13}C)$_2$** employed Fv[W(CO)$_3$Me][Rh(C_2H_4)$_2$] (**9**), that was synthesized according to ref. 5, as the precursor (Scheme 4), since this reaction could be easily monitored by ^1H NMR spectroscopy by the gradual appearance of the signals due to **1-(^{13}C)$_2$** at the expense of those from **9**. Under these conditions (50 psi ^{13}CO, 65°C, 2 days), no intermediates were detected but the reaction most likely proceeded *via* stepwise substitution analogous to that reported for the cyclopentadienyl complex $CpRh(C_2H_4)_2$ [21].

2.5.2. Photo- and thermal chemistry of 1-(^{13}C)$_2$

Unfortunately, when **1-(^{13}C)$_2$** was irradiated in solution, intermolecular label scrambling took place, as detected by mass spectroscopy. Therefore, a matrix isolation experiment, a technique designed to inhibit scrambling processes and detect reactive intermediates by using low temperatures and high dilution conditions [22], was applied. Thus, **1-(^{13}C)$_2$** was deposited in an argon matrix at 12 K, and characterized by the carbonyl stretches in the IR spectrum at 2027, 2006, 1947, and 1939 cm^{-1}. After ten minutes of irradiation with a 1000 W Hg/Xe arc lamp equipped with an interference filter to provide light of wavelengths above 300 nm, **1-(^{13}C)$_2$** was completely consumed and, more importantly, no scrambling of the isotopic label had occurred. Besides the presence of free unlabeled CO (ν(CO) = 2140 cm^{-1}), only one product was evident, giving rise to carbonyl bands at 2008, 1961, 1950, and 1876 cm^{-1}. Based on comparison with the known spectral features of $CpW(CO)_2Me$ (paraffin matrix, 77 K, ν(CO) = 1955, 1861 cm^{-1}) and $CpRh(^{13}CO)_2$ (hexanes, 298 K, ν(CO) = 2000, 1939 cm^{-1}), this new compound was believed to be **11-(^{13}C)$_2$**. Under the constraints of the matrix, **11-(^{13}C)$_2$** did not react further to produce **2-(^{13}C)$_2$** (Scheme 4).

Heating up **1-(^{13}C)$_2$** led to intermolecular label scrambling and did not give a conclusive result. However, **4-(^{13}C)$_1$** was the major component of the resulting mixture, suggestive of a carbonyl loss from rhodium (Scheme 4). Complex **4-(^{13}C)$_1$** could also be prepared by exposing a THF-d_8 solution of **3** to 50 psi of ^{13}CO at 40°C resulting in an increase in the intensity of the doublet in the ^{13}C NMR spectrum centered at 198.20 ppm ($J(^{103}Rh-^{13}C)$ = 83.0 Hz), indicating incorporation of the label at the terminal carbonyl position of the rhodium center (Scheme 4).

2.5.3. Discussion of reaction mechanisms

The reversible transformation of **3** to **4** (Scheme 1) could originate from either the entering carbon monoxide directly inserting into the metal–alkyl bond [23], or *via* a migratory insertion reaction, the pathway commonly invoked in the transformation of a molecule containing adjacent alkyl and carbonyl groups into an acyl complex [20b,24]. Since the labeling experiment showed that the ^{13}CO was selectively incorporated at the terminal positon of the rhodium center (Scheme 4), the formation of the acyl ligand should be viewed as arising from a migratory insertion reaction involving the coordinated CO ligand rather than the direct insertion of the incoming carbon monoxide. It should be noted that the W–CO positions also incorporated the labeled carbon monoxide. However, this tungsten unit is known to exchange CO ligands under similar conditions and most likely does not participate in the insertion reaction.

The transfer of an alkyl group between two transition metals, as observed in the thermal rearrangement of **2** to **3** (Scheme 1), is a relatively uncommon transformation. Methyl–methyl exchange in a Pt/Zr heterobimetallic system constitutes one of the rare examples of such a process [25]. One possible mechanism for the transformation of **2** to **3** is carbonyl migration to tungsten to produce the coordinatively unsaturated rhodium center in **10** (Scheme 5). Insertion of this fragment into the W–Me bond achieves the methyl migration required to produce **3**. The reactivity of **2** with ^{13}CO is also consistent with the presence of **10**, since coordination of the incoming ligand occurs only at the unsatu-

rated rhodium site to produce **1**-$(^{13}C)_1$, which can undergo further exchange to give **1**-$(^{13}C)_2$ (Scheme 4).

Regarding the photoreaction that transformed **1** into **2** (Scheme 1), the cleaved off CO ligand could originate either from the W or the Rh center. However, **1**-$(^{13}C)_2$ gave **11**-$(^{13}C)_2$ upon irradiation (Scheme 4), which argues strongly that **2** derived from photodissociation of a tungsten carbonyl ligand and addition of the unsaturated W center to a Rh–CO bond (Scheme 5).

The mechanism used to explain the thermal reactivity of **1** (Scheme 6) is proposed on direct analogy to the molybdenum system (Scheme 3).

Assuming **6** was indeed an intermediate in the formation of acyl **7**, the thermal dissociation of carbon monoxide was probably not the primary step in the formation of **3** from **1**. In fact, this result implied that the initial product arising from thermolysis of **1** was the acyl-complex **4**, which, under the experimental conditions, decarbonylated to yield **3**. This assumption was corroborated by the thermal reaction of **1**-$(^{13}C)_2$ under mild reaction conditions, which actually gave **4**-$(^{13}C)_1$ (Scheme 4). The greater reactivity for the molybdenum system follows the trends observed for molecules of the type $CpM(CO)_3Me$ (M = Mo, W) [20]; the stronger W–Me bond held responsible for the higher barrier to acyl formation. The key feature in the proposed reaction sequence from **1** to **3** (Scheme 6) is the initial

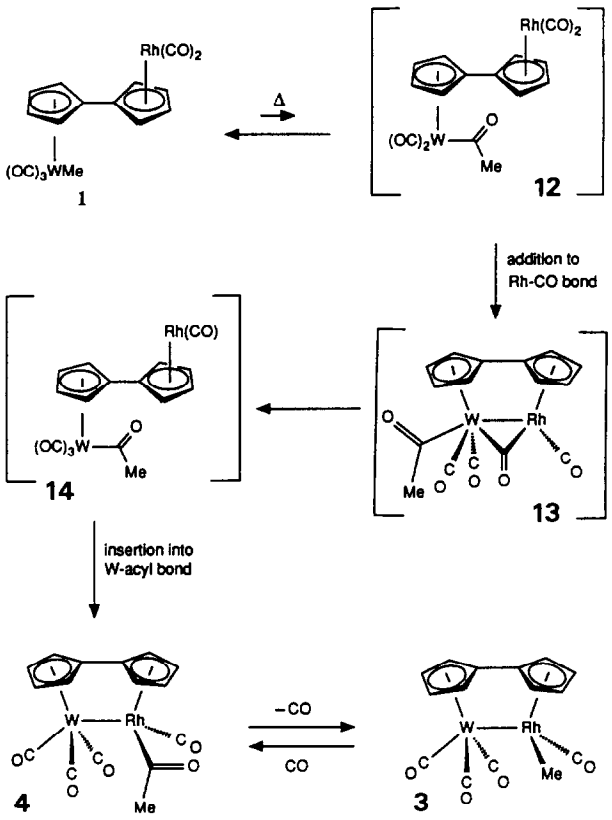

Scheme 6. Proposed mechanism for the transformation of **1** to **3** and **4**.

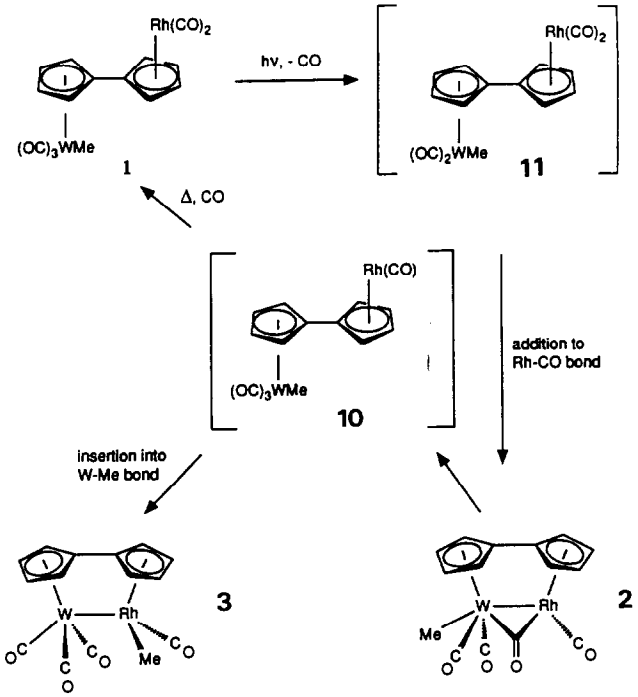

Scheme 5. Proposed mechanisms for the transformations of **1** to **2**, **2** to **1**, and **2** to **3**.

methyl migratory insertion to form the unsaturated acyl intermediate **12**, precedented by the behavior of $CpW(CO)_3Me$ [20]. From this point, the mechanism proceeds by a similar course as that proposed to account for the conversion of **2** to **3**. Under the reaction conditions, the bridging carbonyl complex **13** readily rearranges to **4** *via* **14**. A related acetyl transfer from zirconium to rhodium has been reported [26]. Decarbonylation of the Rh–acyl **4** produces the observed product from this reaction, **3**. The observation that **1**-$(^{13}C)_2$ lost one ^{13}CO ligand upon heating (Scheme 4) further corroborated the suggested reaction pathway, especially with respect to carbonyl loss from rhodium.

2.6. Phosphine induced heterobimetallic zwitterion formation

Like many acyl producing migratory insertion reactions [20b,24], the carbonylation of the alkyl group in **3** was shown to be promoted by the incoming CO ligand (Scheme 1). Many types of Lewis bases can serve as the external ligand, a much studied example being a tertiary phosphine. Therefore, to test the generality of the conversion of **3** to **4**, the reactivity employing PMe_3 as the incoming ligand was explored.

Exposure of a red solution of **3** to a tenfold excess of PMe_3 for 5 h at room temperature, resulted in the gradual formation of an orange precipitate of **16** (Scheme 7). Using one equivalent of phosphine also gave **16**, but with poor yield. Thus, instead of promoting the migratory insertion reaction leading to the formation of **15**, the PMe_3 had attacked the rhodium center to produce the heterodinuclear zwitterion **16**, analogous to the reactivity of $FvM_2(CO)_6$ (M = Mo, W) [27] in the presence of this phosphine. That we were unable to obtain **15** may reflect the strain imposed on the system by the bent fulvalene ligand, rendering the metal–metal bond more susceptible to heterolysis in the presence of a strong nucleophile.

The most revealing feature in the ^1H NMR spectrum of **16** was the doublet of triplets centered at 0.31 ppm, indicating that the methyl group was coupled to ^{103}Rh ($J(^{103}Rh-^{13}C) = 2.3$ Hz) and two ^{31}P nuclei ($J(^{31}P-^1H) = 5.3$ Hz). In addition, the carbonyl stretching frequencies had decreased, as compared with **1**, to 1898 and 1787 cm^{-1}, a consequence of the greater degree of backbonding from the anionic tungsten center. $[CpW(CO)_3]^-[Na]^+$ exhibits similar bands at 1894 and 1787 cm^{-1} [28]. The limited solubility of **16** in common organic solvents and the presence of two magnetically active nuclei (^{103}Rh and ^{31}P, both 100% natural abundance) precluded the acquisition of a complete ^{13}C NMR spectrum, so the peaks corresponding

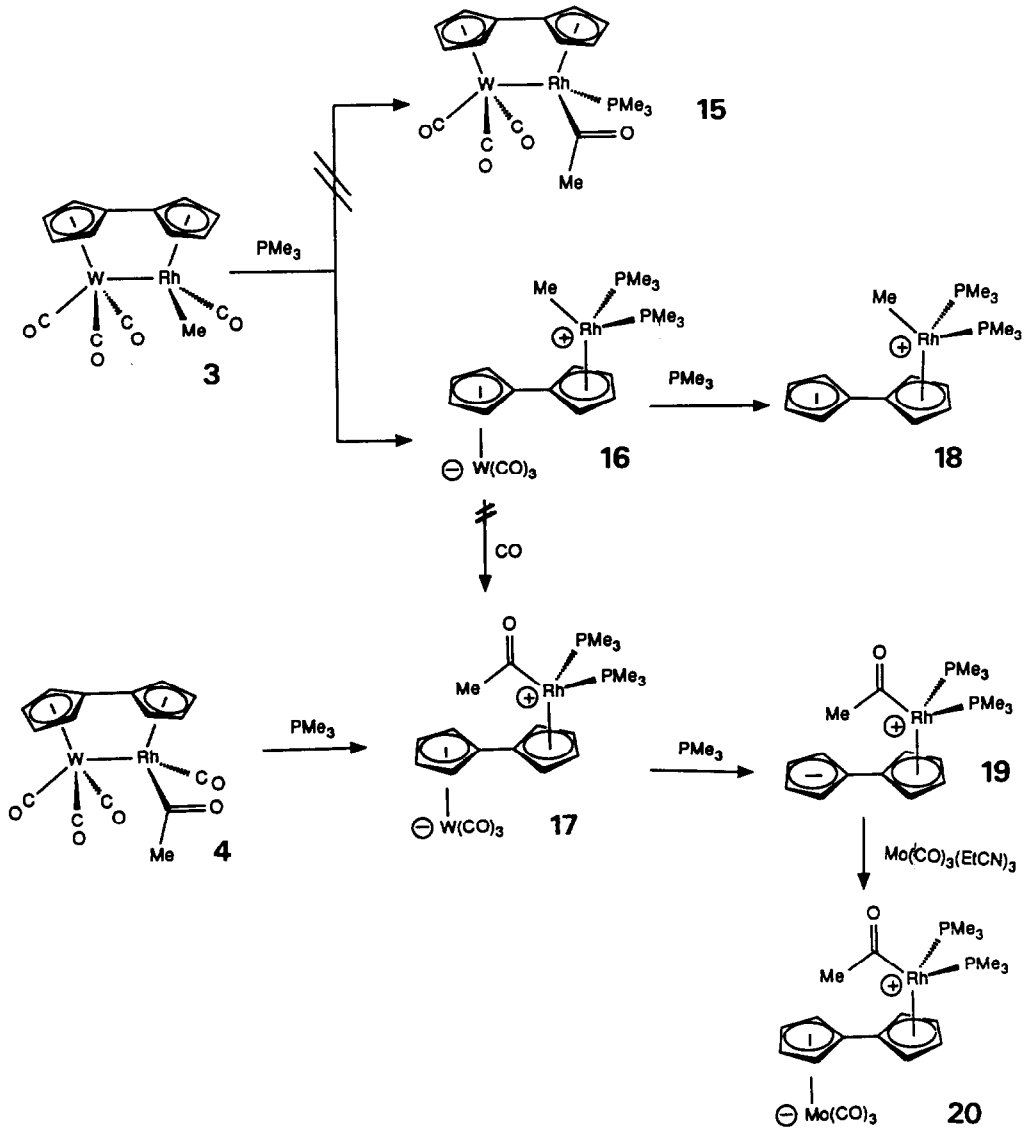

Scheme 7. Reactions of fulvalene complexes containing W and Rh with PMe_3.

to the quaternary fulvalene and methyl carbons could not be observed. A signal at 226.32 ppm was consistent with the tungsten carbonyl carbons, the W–CO peaks for $[CpW(CO)_3]^-[Na]^+$ appearing at 226.7 ppm [29]. The ^{31}P NMR spectrum displayed a doublet centered at 5.95 ppm with a ^{31}P–^{103}Rh coupling constant of 144.5 Hz.

Complex **16** could not be carbonylated to the zwitterionic acyl **17** under CO (50 psi) at 100°C. One of the requirements for a migratory insertion reaction is that the groups undergoing the transformation should occupy adjacent positions in the coordination sphere of the metal [24], as exemplified by the methyl and CO ligands in **3**. This requirement is not fulfilled by **16**. But **17** could be prepared independently by the reaction of **4** with PMe_3 (Scheme 7). This transformation proceeded in a manner similar to that observed for **3**, although at a much greater rate, resulting in a 90% yield of **17** after only 30 min. The rate enhancement could be attributed to the electron withdrawing ability of the acyl group, rendering the metal center more susceptible to nucleophilic attack by the phosphine.

The spectral and analytical data of **17** supported the assigned structure. The ^{31}P NMR spectrum exhibited the expected doublet at 4.69 ppm ($J(^{103}Rh-^{31}P) = 157.2$ Hz) while the carbonyl stretching frequencies in the IR spectrum occurred at 1890, 1763, and 1639 cm^{-1}, the latter attributed to the acyl moiety [4]. As with **3**, the ^{13}C NMR spectrum displayed a signal at 225.90 ppm, indicative of the anionic tungsten unit. Peaks at 2.41 ppm and 49.92 ppm, from ^1H NMR and ^{13}C NMR spectroscopy, respectively, derived from the acyl–methyl group. Unequivocal proof of the formulation was obtained from an X-ray structure analysis of crystals obtained by slow diffusion of C_6H_6 into a CH_3CN solution of **17**. An ORTEP drawing is shown in Fig. 2 and bond length and angle data can be found in the supplementary material. The separation between the two Cp rings of the fulvalene ligand is 1.453(9) Å, similar to that found for **4** (1.454(17) Å), reflecting single bond character. The average W–CO bond length of 1.926 Å is decreased relative to **4** (1.984 Å) as a result of the increased backbonding from the anionic tungsten center. This effect is also observed as a lengthening of the corresponding C–O separation from an average of 1.139 Å (**4**) to 1.170 Å (**17**). The bonding parameters for the acyl moiety are analogous to those found in **4**.

The behavior of **3** and **4** in the presence of PMe_3 (Scheme 7) is reminiscent of the reactions of the homodinuclear Ru, Mo, and W fulvalene complexes [27,30]. In this case, however, two different metal centers are present, yet the attack of the phosphine proceeds with remarkable selectivity. A similar metal-

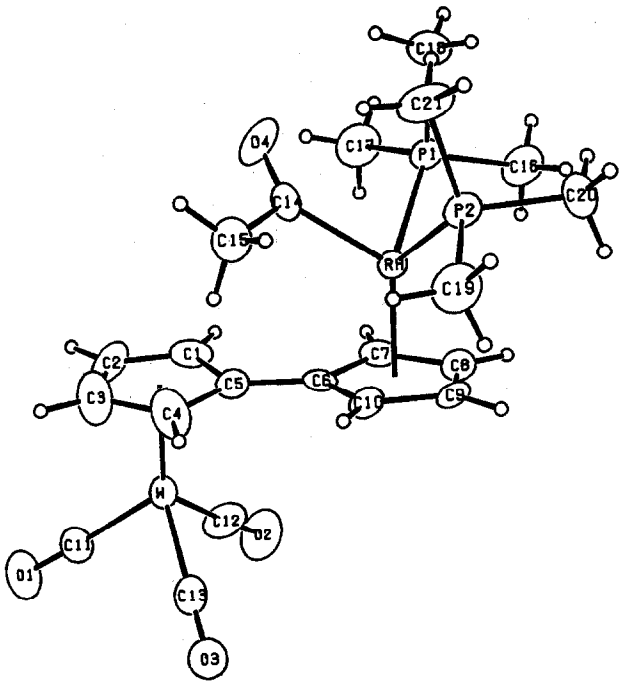

Fig. 2. ORTEP drawing of $Fv(CO)_3WRh(PMe_3)_2C(O)Me$ (**17**). Bond length and angle data are given in the text and in the supplementary material.

specific attack of the phosphine was observed for $FvMoRu(CO)_5$, resulting in decomplexation of the molybdenum half of the fulvalene ring to yield ring-slipped $FvRu(CO)_2PMe_3$ [1,31,32]. A possible explanation invokes a steric effect, namely it might be that the lower coordination number about the rhodium site facilitates the approach of the PMe_3. On the other hand, the transformation of **3** and **4** to their respective zwitterions involves oxidation of the more electron-rich Rh^{II} (d^7) center to Rh^{III} (d^6) with concomitant reduction of W^I (d^5) to W^0 (d^6), suggesting that the metal-specificity derives from kinetic or thermodynamic electronic factors.

In analogy to the chemistry observed for the dimolybdenum zwitterions [9], both **16** and **17** reacted further with an excess of PMe_3 at room temperature in CH_3CN, producing mononuclear **18** and **19**, respectively (Scheme 7). The polar solvent was necessary for the reaction to occur, the zwitterions being unreactive with the phosphine in solvents in which they did not dissolve (THF, for example). Unfortunately, purification of these compounds proved impossible since their solubility properties were quite similar to those of the by-product, *fac*-$W(CO)_3(PMe_3)_3$. Therefore, they were characterized only by NMR spectroscopy. For example, a CD_3CN solution of **16** was sealed in an NMR tube with a large excess of PMe_3 (> 8 equivalents) and allowed to sit overnight. The reaction mixture turned

from orange to red. The ^{31}P NMR spectrum exhibited a doublet centered at 2.48 ppm, the peaks separated by 150.5 Hz due to coupling to the ^{103}Rh nucleus. The resonance arising from the *fac*-$W(CO)_3(PMe_3)_3$ appeared at −41.25 ppm surrounded by satellites with a $^{31}P-^{183}W$ coupling constant of 218 Hz [33]. In addition, the ^1H NMR spectrum contained the six expected peaks required for **18**, the protons of the methyl group coupled to both ^{103}Rh (2.4 Hz) and ^{31}P (6.2 Hz). The related acyl complex, **19**, was produced and characterized in a similar manner. Analysis by ^{31}P NMR spectroscopy revealed a doublet centered at 1.69 ppm ($J(^{103}Rh-^{31}P) = 164$ Hz) while the ^1H NMR spectrum exhibited the expected six signals, the singlet at 2.30 ppm being characteristic of the acyl moiety.

Further evidence for the structure of **19** was gained by taking advantage of the fact that the mononuclear product and *fac*-$W(CO)_3(PMe_3)_3$ were soluble in THF while the heterobimetallic zwitterions would only dissolve in more polar solvents like CH_3CN. Exposure of a THF solution of **19** to $Mo(CO)_3(EtCN)_3$ resulted in recomplexation of the free Cp ring in **19**, giving the orange solid **20** (Scheme 7). The spectral features of this material were very similar to those of **17**. The IR spectrum displayed carbonyl stretching absorptions at 1892, 1773, and 1636 cm^{-1} while the acyl–methyl group resonated at 2.41 ppm and 50.10 ppm in the ^1H and ^{13}C NMR spectra, matching the peaks for **17** almost identically. However, the ^{13}C NMR spectrum exhibited a signal at 235.22 ppm, assigned to the carbonyl carbons at molybdenum. The analogous carbons in $[CpMo(CO)_3]^-[Na]^+$ resonate at 236.6 ppm [34]. As with **16**, the peaks derived from the quaternary carbons attached to rhodium could not be detected, due primarily to the limited solubility of the complex and the coupling to ^{103}Rh and two ^{31}P nuclei, decreasing the intensity of the signal. An adequate elemental analysis could not be obtained because the solvents used for the recrystallization (C_6H_6 and CH_3CN) remained in the crystalline lattice. Mass spectral analysis confirmed the assigned formulation by the presence of a molecular ion at $m/z = 608$. Thus, the structural assignment of **19**, and by analogy, **18**, is most likely correct. In addition, the formation of **20** bodes well for the construction of other heterodinuclear zwitterions containing rhodium.

3. Conclusions

In the course of this work we could synthesize and fully characterize several new heterobimetallic W, Rh– and Mo, Rh–fulvalene complexes. The mechanisms of their photo- and thermal chemistry could be elucidated by ^{13}C labeling experiments: while it is the W site that loses a CO ligand when the starting material **1** is irradiated, under thermal conditions the Rh site is the CO donating part.

On the whole, the W, Rh fulvalene complexes differed in photo- and thermal reactivity from comparable Cp compounds as well as from their corresponding homodinuclear analogs. One of the unique reaction features observed was methyl migration from tungsten to rhodium. Reactions of fulvalene complexes containing W and Rh with PMe_3 were completely site-specific, the ligand attacked selectively the rhodium moiety of the molecule. To sum it up, heterodinuclear fulvalene complexes display unique and novel reactivity that can be fine tuned by using different metal combinations.

4. Experimental details

4.1. General remarks

Unless specifically stated otherwise, all manipulations were performed under an atmosphere of purified Ar or N_2, either in a Vacuum Atmospheres Inc. glovebox or using standard Schlenk and vacuum line techniques. All solvents were dried and degassed by standard procedures. The compounds **1** [5], **5** [35], and **9** [5] were prepared as described in the given literature.

Photoreactions of **1** were performed in a Pyrex tube using a Rayonet Model RPR-100 photochemical reactor equipped with lamps having a primary radiation output of a wavelength range centered around 300 nm. Irradiation of **1-($^{13}C)_2$** was accomplished with a Candela model UV1050 coaxial flashlamp tunable dye laser, operating with a 2×10^{-5} M ethylene glycol solution of rhodamine 590 laser dye, tuned to a wavelength of 306 nm.

^1H NMR spectra were recorded on a Bruker AMX 400 or AM 400 and on a U.C. Berkeley 300 MHz instrument equipped with a Cryomagnets Inc. magnet and a Nicolet Model 1280 data collection system. ^1H NMR spectra are reported as follows: chemical shift in ppm downfield of tetramethylsilane using the residual proton resonance of the deuterated solvent as an internal standard. The AA′XX′ patterns of symmetrical fulvalene (Fv) ligands are reported as multiplets. The $AA'X_9X'_9M$ spin system of two *cis* PMe_3 ligands bound to Rh is reported as "doublet of doublets" with a $J(^{31}P-^1H)$ coupling constant equal to the frequency difference between the outer lines representing the sum of $^2J(^{31}P-^1H)$ and $^4J(^{31}P-^1H)$.

^{13}C NMR spectra were recorded with proton decoupling on the U.C. Berkeley 300 MHz instrument or a Bruker AM-400 or AMX 400 instrument operating at 75 and 100 MHz, respectively. ^{13}C NMR chemical shifts are reported relative to tetramethylsilane using the deuterated solvent resonances as internal stand-

ards. The resonance due to the carbons in $Rh(PMe_3)_2$ moieties is reported as a "triplet" with a coupling constant equal to the frequency difference between the two outer lines representing the sum of $^1J(^{31}P-^1H)$ and $^3J(^{31}P-^1H)$. ^{31}P NMR spectra were recorded with proton decoupling on the U.C. Berkeley 300 MHz instrument operating at 121.5 MHz. ^{31}P NMR shifts are reported relative to an external standard of 85% H_3PO_4 in CD_3CN.

Infrared spectra were recorded on a Perkin-Elmer Model 681 spectrophotometer equipped with a 580 B Data Station; only the most intense peaks in the spectrum are reported. Electronic spectra were recorded on a Perkin-Elmer Model 8450A UV-Visible Diode Array spectrophotometer. Mass spectra were acquired by the U.C. Berkeley Mass Spectrometry Laboratory on AEI-MS12, Finnigan 4000, or Kratos MS50 instruments. Fast Atom Bombardment (FAB) mass spectra were obtained using sulfolane, nitrobenzylalcohol (NBA), or nitrophenyl octyl ether (NPOE) as solvent. The natural isotopic distribution of the transition metals (W, Mo, etc.) produced broad peak envelopes; only the most intense peak of each fragment is reported. Elemental analyses were performed by the U.C. Berkeley Microanalytical Laboratory. Melting points were measured on a Thomas Hoover Unimelt apparatus in glass capillary tubes sealed under argon and are uncorrected.

Infrared spectra for the matrix isolation experiment [22] were recorded with an IBM IR44 FTIR instrument equipped with a globular source, Ge-coated KBr beam splitter, and liquid nitrogen cooled Hg/Cd/Te detector. Spectra were collected between 4000 and 400 cm^{-1} with a resolution of 0.5 cm^{-1}. The sample of **1-(^{13}C)$_2$** was codeposited with Ar onto a CsI target cooled to 12 K by an Air Products Displex Model CSA-202 closed-cycle helium refrigerator supplied with a Au (0.07% Fe) *vs.* chromel thermocouple and a resistance heater. The expander was mounted such that a rotation of 90° placed the matrix in the optical path of the FTIR spectrometer. A further rotation permitted photolysis of the sample by a Hanovia Model 6140 lamp housing equipped with a 2 inch $f/1.0$, UV-grade fused silica, two element, focusing lens and a cooled 3 inch water filter with quartz windows. An Optics Technology Inc. Model 297 nm Interference Filter was used to select wavelengths > 300 nm.

4.2. *Fv(CO)$_2$MeWRh(CO)[μ-CO] (2)*

A Pyrex tube containing a deoxygenated solution of **1** (96 mg, 0.168 mmol) in THF (100 ml) was placed in a water cooled quartz immersion well and irradiated using the Rayonet Photochemical Reactor for 45 min. The solvent was removed under vacuum and the residue applied in air to the top of a column of silica gel using THF–hexanes (7:3). THF–hexanes (1:9) eluted a yellow band which was collected and the solvent removed to recover unreacted **1** (11 mg, 0.019 mmol). A gradient of THF–hexanes (3:7 to 1:1) led to an orange band which was collected and the solvent removed under vacuum. Recrystallization of the residue by diffusion of hexanes vapor into an acetone solution afforded air-stable **2** (50 mg, 55% based on recovered starting material): orange flakes, m.p. 148–150°C; ^1H NMR (300 MHz, THF-d_8, −60°C) δ 6.37 (m, 1 H), 6.15 (m, 1 H), 6.06 (m, 1 H), 5.94 (m, 1 H), 5.86 (m, 1 H), 5.33 (m, 1 H), 4.97 (m, 1 H), 4.45 (m, 1 H), 0.35 (s, 3 H); ^{13}C NMR (75 MHz, THF-d_8, −60°C) δ 246.89 (d, $J(^{103}Rh-^{13}C) = 37$ Hz), 219.32, 209.98, 194.54 (d, $J(^{103}Rh-^{13}C) = 93$ Hz), 110.94, 97.83, 95.89, 95.46, 95.31, 90.59, 89.77, 86.09, 84.22, 83.32, −18.84 (coupling of ^{103}Rh to the fulvalene carbons was not observed); IR (THF) ν(CO) 2008, 1967, 1905, 1775 cm^{-1}; mass spectrum, *m/e* (rel intensity) 542 (M^+, 31.8), 514 (M^+–CO, 25.4), 484 (M^+–2CO, 71.0), 456 (M^+–3CO, base), 428 (M^+–4CO, 79.8), 413 (M^+–2CO–CH_3, 78.8). Anal. Calcd. $C_{15}H_{11}O_4RhW$: C, 33.24; H, 2.04. Found: C, 33.51; H, 2.24.

4.3. *Fv[W(CO)$_3$Me][Rh(^{13}CO)$_2$] (1-(^{13}C)$_2$)*

4.3.1. *Method A*

A solution of **2** (10 mg, 0.018 mmol) in THF-d_8 was placed in a high pressure NMR tube equipped with a Teflon valve and degassed by three freeze–pump–thaw cycles. The tube was pressurized with ^{13}CO (50 psi), sealed, and heated to 45°C for 17 h. The reaction mixture was treated as described for **2** affording **1-(^{13}C)$_2$** (5 mg, 47%): IR (hexanes) ν(CO) 2014, 2001, 1945, 1933 cm^{-1}; mass spectrum, *m/e* (rel. intensity) Calcd. for $C_{14}H_{11}^{13}C_2O_5RhW$: 576 (1.8), 575 (13.5), 574 (87.0), 573 (15.4), 572 (M^+, 100), 571 (55.4), 570(78.9); Found: 576 (21.2), 575 (11.5), 574 (89.3), 573 (29.2), 572 (M^+, 100), 571 (44.4), 570 (60.0).

4.3.2. *Method B*

A stainless steel Paar bomb was loaded with a solution of **1** (79 mg, 0.138 mmol) in acetone (15 ml). The apparatus was cooled to −78°C, evacuated, and pressurized with ^{13}CO (50 psi). The solution was then heated to 45°C for 1 day. An infrared spectrum (hexanes) of an aliquot of the reaction mixture revealed, in addition to the absorbances attributed to **1-(^{13}C)$_2$**, carbonyl stretches at 2032, 2015, 1961, and 1934 cm^{-1}, assigned to **1-(^{13}C)$_1$**. Continued heating under a new charge of ^{13}CO (50 psi) for an additional 3 days afforded **1-(^{13}C)$_2$** (55 mg, 70%).

4.3.3. Method C

A solution of **9** (49 mg, 0.086 mmol) in THF-d_8 was placed in a high pressure NMR tube equipped with a Teflon valve and degassed by three freeze–pump–thaw cycles. The tube was pressurized with ^{13}CO (50 psi), and heated to 65°C for 2 days. The reaction mixture was treated as described for **2** affording **1**-$(^{13}C)_2$ (30 mg, 61%).

4.4. $Fv(CO)_3WRh(CO)CH_3$ (3)

4.4.1. Method A

A solution of **1** (214 mg, 0.375 mmol) in toluene (25 ml) was heated to reflux for 24 h. The solvent was removed under vacuum and the residue applied in air to the top of a column of silica gel using THF–hexanes (1:1). Eluting first with THF–hexanes (1:9) produced a yellow band of **1** which was discarded. Further elution with THF–hexanes (3:7) produced a red band that was collected and the solvent removed under vacuum. Recrystallization of the residue by diffusion of hexanes vapor into a THF solution afforded air-stable crystals of **3** (148 mg, 70%): red crystals, m.p. 217–220°C (dec.); ^1H NMR (300 MHz, THF-d_8) δ 6.12 (m, 1 H), 5.84 (m, 1 H), 5.59 (m, 1 H), 5.37 (m, 1 H), 5.05 (m, 1 H), 4.77 (m, 1 H), 4.47 (m, 1 H), 4.37 (m, 1 H), 0.68 (d, $J(^{103}Rh-^{13}C = 2.5$ Hz); ^{13}C NMR (75 MHz, THF-d_8, −60°C) δ 225.02, 211.97, 211.84, 198.20 (d, $J(^{103}Rh-^{13}C) = 83.0$ Hz), 97.84 (d, $J(^{103}Rh-^{13}C) = 0.9$ Hz), 96.14 (d, $J(^{103}Rh-^{13}C) = 2.4$ Hz, 95.42 (d, $J(^{103}Rh-^{13}C) = 3.8$ Hz), 94.71, 86.21 (d, $J(^{103}Rh-^{13}C) = 2.1$ Hz, 85.75, 85.34 (2C), 85.23 (d, $J(^{103}Rh-^{13}C) = 3.9$ Hz), 83.91, −20.62 (d, $J(^{103}Rh-^{13}C) = 24.4$ Hz); IR (THF) ν(CO) 2010, 1965, 1895 cm^{-1}; mass spectrum *m/e* (rel. intensity) 542 (M^+, 26.5), 514 (M^+–CO, 20.8), 484 (M^+–2CO, 61.0), 456 (M^+–3CO, 58.3), 428 (M^+–4CO, 54.4), 413 (M^+–2CO–CH_3, 88.3), 40 (base); UV-VIS (THF): λ_{max} (log ϵ) 300 (4.07), 357 (sh, 3.60), 418 (3.70), 528 (3.06) nm. Anal. Calcd. for $C_{15}H_{11}O_4RhW$: C, 33.24; H, 2.04. Found: C, 33.54; H, 2.10.

4.4.2. Method B

A solution of **2** (20 mg, 0.037 mmol) in toluene (10 ml) was brought to reflux for 24 h. The reaction mixture was treated as above affording **3** (12 mg, 60%).

4.4.3. Method C

A solution of **4** (10 mg, 0.017 mmol) in toluene (10 ml) was brought to reflux for 6 h. The reaction mixture was treated as above affording **3** (8 mg, 84%).

4.5. $Fv(CO)_3WRh(CO)C(O)CH_3$ (4)

A solution of **3** (43 mg, 0.079 mmol) in THF (5 ml) was placed in a glass bomb equipped with a Teflon valve and degassed using three freeze–pump–thaw cycles. The bomb was sealed under CO (1 atm) and placed in an oil bath at 45°C for 24 h. The solvent was removed under vacuum and the residue applied in air to the top of a column of silica gel using THF–hexanes (3:1). Eluting with THF–hexanes (3:7) produced a red band that was collected and the solvent removed under vacuum. Recrystallization of the residue by diffusion of hexanes vapor into a THF solution afforded air-stable crystals of **4** (40 mg, 89%): red crystals, m.p. 177–178°C; ^1H NMR (300 MHz, THF-d_8) δ 6.19 (m, 1 H), 6.11 (m, 1 H), 5.69 (m, 1 H), 5.45 (m, 1 H), 5.12 (m, 1 H), 4.83 (m, 1 H), 4.33 (m, 1 H), 4.08 (m, 1 H), 2.51 (s, 3 H); ^{13}C NMR (75 MHz, THF-d_8) δ 225.92 (d, $J(^{103}Rh-^{13}C) = 30.8$ Hz), 223.88, 213.85, 211.48, 196.70 (d, $J(^{103}Rh-^{13}C) = 92.3$ Hz), 101.36, 97.06 (d, $J(^{103}Rh-^{13}C) = 1.4$ Hz), 96.19, 95.64 (d, $J(^{103}Rh-^{13}C) = 4.5$ Hz), 93.01 (d, $J(^{103}Rh-^{13}C) = 5.0$ Hz), 85.97, 85.54, 85.38, 84.91, 84.65, 50.47 (d, $J(^{103}Rh-^{13}C) = 4.3$ Hz); IR (KBr) ν(CO) 2011, 1965, 1905, 1879, 1635 cm^{-1}; FAB-mass spectrum (NBA) 571 (MH^+); UV-VIS (THF): λ_{max} (log ϵ) 261 (4.20), 288 (4.17), 397 (3.92), 528 (2.97) nm. Anal. Calcd. for $C_{16}H_{11}O_5RhW$: C, 33.71; H, 1.94. Found: C, 33.60; H, 1.99.

Preparation of **4** using ^{13}CO: a solution of **3** (11 mg, 0.020 mmol) was placed in a high pressure NMR tube equipped with a Teflon valve and degassed using three freeze–pump–thaw cycles. The tube was pressurized with ^{13}CO (50 psi), sealed, and heated to 40°C for 24 h. Analysis by ^{13}C NMR spectroscopy revealed incorporation of the label into the W–CO (223.88, 213.85, and 211.48 ppm) and terminal Rh–CO (196.70 ppm) positions, observed as an increase in the intensity of the respective signals.

4.6. X-ray diffraction analysis of 4

X-ray quality crystals were grown by diffusion of hexanes vapor into a solution of **4** in THF. Crystal size $0.18 \times 0.19 \times 0.31$ mm^3, space group $P\bar{1}$, $a = 13.529(3)$ Å, $b = 15.813(3)$ Å, $c = 16.164(3)$ Å, $\alpha = 62.72(1)°$, $\beta = 87.24(1)°$, $\gamma = 86.32(1)°$, $V = 3065.9(11)$ $Å^3$, $Z = 8$, $\mu = 8.74$ mm^{-1}, $d_{calcd} = 2.470$ g cm^{-3}, radiation: Mo K_α ($l = 0.71069$ Å), 2θ-range: $3° \leqslant 2\theta \leqslant 45°$, scan mode: ω, scan range in ω: 0.8°, temperature: 120 K, reflections collected: 8020, reflections observed: 7255 [$F_o \geqslant 4\sigma(F)$], $R = 0.037$, $R_w = 0.045$. Atomic coordinates and anisotropic atomic displacement factors are listed in the supplementary material.

4.7. $Fv(CO)_3MoRh(CO)C(O)CH_3$ (7)

A solution of **5** (190 mg, 0.586 mmol) in THF (20 ml) was treated with a slight excess of NaH. After stirring for about 15 min the deprotonation was complete, as judged by the ceasing H_2 evolution. Excess NaH was

removed by filtration prior to the addition of $[(CO)_2RhCl]_2$ (150 mg, 0.293 mmol). After stirring for 3 h and removal of the solvent, the residue was extracted with ether and brought on top of a column packed with silica gel. Ether-pentanes (1:1) eluted a red zone. Removal of the solvent gave a red powder, that was recrystallized by slow diffusion of hexanes into a THF solution of **7**: red crystals, m.p. 162°C (dec.), (0.05 mg, 0.104 mmol, 18%). ^{1}H NMR (400 MHz, C_6D_6) δ 5.37 (m, 1 H), 5.05 (m, 1 H), 4.63 (m, 1 H), 4.24 (m, 1 H), 3.81 (m, 1 H), 3.76 (m, 1 H), 3.74 (m, 1 H), 2.87 (m, 1 H), 2.66 (s, 3 H); ^{1}H NMR (400 MHz, THF-d_8) δ 6.12, 6.08, 5.72, 5.44, 4.97, 4.62, 4.25, 3.98, 2.53 (multiplicities and integrals as above). ^{13}C NMR (100 MHz, THF-d_8) δ 226.83 ($J(^{103}Rh-^{13}C) = 30.4$ Hz), 197.43 ($J(^{103}Rh-^{13}C) = 93.4$ Hz), 101.46, 100.25, 95.81, 89.38 ($J(^{103}Rh-^{13}C) = 4.8$ Hz), 92.90 ($J(^{103}Rh-^{13}C) = 4.8$ Hz), 88.26, 88.08, 87.50, 87.11, 85.33 ($J(^{103}Rh-^{13}C) = 1.94$ Hz), 50.48 ($J(^{103}Rh-^{13}C) = 3.8$ Hz); mass spectrum m/e (rel. intensity) 484 (M^+, 30.0), 456 (M^+–CO, 23.4), 428 (M^+–2CO, 23.6), 413 (M^+–2CO–CH_3, 4.1), 385 (M^+–3CO, 5.0), 302 (M^+–$Mo(CO)_3$, 12.0), 43 ($COCH_3$, 100); IR (KBr) ν(CO) 2015, 1967, 1891, 1887, 1631; UV–VIS (THF) λ_{max} (log ϵ) 530 (3.04), 402 (3.99), 275 (4.23), 288 (4.21); Anal. Calcd. for $C_{16}H_{11}O_5MoRh$: C, 39.86; H, 2.30. Found: C, 40.25; H, 2.81.

4.8. $Fv(CO)_3MoRh(CO)CH_3$ (8)

A solution of **7** (150 mg, 0.311 mmol) in diglyme was refluxed for 3 h. After removal of the solvent the residue was purified as above. Brown crystals of **8** (134 mg, 0.295 mmol, 95%) were obtained by slow diffusion of hexanes into an THF solution of **8**. M.p. 170°C (dec.); ^{1}H NMR (400 MHz, C_6D_6) δ 5.02 (m, 1 H), 4.87 (m, 1 H), 4.64 (m, 1 H), 4.38 (m, 1 H), 3.83 (m, 1 H), 3.43 (m, 1 H), 3.28 (m, 1 H), 3.21 (m, 1 H), 0.94 (d, $J(^{103}Rh-^1H) = 2.6$ Hz), 3 H); ^{1}H NMR (400 MHz, THF-d_8) δ 6.04, 7.80, 5.62, 5.38, 4.91, 4.58, 4.37, 4.30, 0.69 (multiplicities and integrals as above); ^{13}C NMR (100 MHz, THF-d_8) δ 100.53, 98.61 ($J(^{103}Rh-^{13}C) = 2.3$ Hz), 97.32, 95.09 ($J(^{103}Rh-^{13}C) = 3.8$ Hz), 93.96, 87.75 ($J(^{103}Rh-^{13}C) = 3.0$ Hz), 86.42, 85.47 ($J(^{103}Rh-^{13}C) = 2.5$ Hz), 84.69 ($J(^{103}Rh-^{13}C) = 4.1$ Hz), −20.31 ($J(^{103}Rh-^{13}C) = 24.3$ Hz); mass spectrum m/e (rel. intensity) 456 (M^+, 18.4), 428 (M^+–CO, 40.2), 413 (M^+–CO–CH_3, 5.3), 385 (M^+–2CO–CH_3, 7.7), 372 (M^+–3CO, 100); IR (KBr) ν(CO) 2005, 1955, 1896, 1878; UV-VIS (THF) λ_{max} (logϵ) 532 (3.48), 426 (4.08), 307 (4.41), 237 (4.57); Anal. Calcd. for $C_{15}H_{11}O_4MoRh$: C, 39.68; H, 2.44. Found: C, 39.41; H, 2.39.

4.9. Photolysis of 1-(^{13}C)$_2$

A solution of **1-(^{13}C)$_2$** (14 mg, 0.024 mmol) in THF-d_8 was placed in an NMR tube and degassed by three freeze–pump–thaw cycles. The tube was sealed under vacuum, placed in a water-cooled quartz well and irradiated for 135 min with a coaxial flashlamp tunable dye laser operating at 306 nm. The reaction mixture was treated as described for **2**. Mass spectral analysis of the recovered product **2-(^{13}C)$_X$** by deconvoluting the observed relative ion intensities of the molecular ion envelope using the simulated spectra for $C_{(15-X)}{}^{13}C_XH_{11}O_4RhW$ indicated the following composition (X, %): (0, 15); (1, 37); (2, 34); (3, 10); (4, 4).

4.10. Photolysis of 1-(^{13}C)$_2$ in an argon matrix, Fv[W(CO)$_2$Me][Rh(^{13}CO)$_2$] (11-(^{13}C)$_2$)

A sample of **1-(^{13}C)$_2$** was deposited in an argon matrix (1.35 mmol, 12 K) by sublimation (80°C, 4.75 h) giving rise to carbonyl stretching frequencies at 2027, 2006, 1947, and 1939 cm^{-1}. The sample was irradiated ($\lambda > 300$ nm) for 10 min producing free ^{12}CO (ν(CO) = 2140 cm^{-1}) and **11-(^{13}C)$_2$**: IR(Ar) ν(CO) 2008, 1961, 1950, 1879 cm^{-1}.

4.11. Thermolysis of 1-(^{13}C)$_2$

A Schlenk flask was charged with a deoxygenated solution of **1-(^{13}C)$_2$** (13 mg, 0.023 mmol) in toluene (25 ml). The solution was brought to reflux for 24 h with an argon purge to expell any liberated carbon monoxide. The reaction mixture was treated as described for **2**. Mass spectral analysis of the recovered product **4-(^{13}C)$_X$** by deconvoluting the observed relative ion intensities of the molecular ion envelope using simulated spectra for $C_{15-X}{}^{13}C_XH_{11}O_4RhW$ indicated the following composition (X, %): (0, 21); 1, 38); (2, 21); (3, 13); (4, 7).

4.12. Fv[W(CO)$_3$][Rh(PMe$_3$)$_2$CH$_3$] (16)

A Schlenk flask was charged with a deoxygenated solution of **3** (25 mg, 0.046 mmol) in THF (15 ml). As the reaction mixture was purged with a stream of Ar, PMe_3 (18 μl, 0.177 mmol) was added *via* syringe resulting in the slow formation of an orange precipitate. After stirring for 5 h under continued gas purge, the solvent was evaporated under vacuum. In the glovebox, the residue was washed with THF to remove unreacted **3** leaving an orange solid that was dissolved in CH_3CN and filtered through a plug of celite. Crystallization of the residue by diffusion of C_6H_6 into a CH_3CN solution afforded air-sensitive **16** with CH_3CN (1:1) (10 mg, 33%): orange crystals, m.p. 240–242°C (dec.); ^{1}H NMR (300 MHz, CD_3CN) δ 5.47 ("t", $J = 2.4$ Hz, 2 H), 5.36 (m, 2 H), 5.27 (m, 2 H), 5.11 ("t", $J = 2.4$ Hz, 2 H), 1.47 ("dd", $J(^{31}P-^1H) = 10.7$ Hz, $J(^{103}Rh-^1H) = 0.9$ Hz, 18 H), 0.31 (dt, $J(^{31}P-^1H) = 5.3$ Hz, $J(^{103}Rh-^1H) = 2.3$ Hz, 3 H); ^{13}C NMR (100 MHz,

CD_3CN) δ 226.32, 92.13 (br), 86.05, 85.59, 84.23 (br), 19.57 ("t", $J(^{31}P-^{13}C) = 34.3$ Hz), (quaternary carbons and $^{103}Rh-CH_3$ were not observed); ^{31}P NMR (121.5 MHz, CD_3CN) δ 5.95 (d, $J(^{103}Rh-^{31}P = 144.5$ Hz); IR (KBr) ν(CO) 1898, 1787 cm^{-1}; FAB-MS (NBA), m/z 666 (M^+), 398 ($M^+-W(CO)_3$). Anal. Calcd. for $C_{20}H_{29}O_3P_2RhW(CH_3CN)$: C, 37.34; H, 4.53; N, 1.98. Found: C, 37.47; H, 4.69; N, 1.66.

4.13. Attempted carbonylation of 16

A high pressure NMR tube equipped with a Teflon valve was charged with **16** (5 mg, 0.007 mmol) in CD_3CN, pressurized with CO (20 psi), and placed in a 100°C oil bath. Periodic monitoring by ^1H NMR spectroscopy revealed only resonances due to **16**.

4.14. Fv[W(CO)$_3$][Rh(PMe$_3$)$_2$C(O)CH$_3$] (17)

A Schlenk flask was charged with a deoxygenated solution of **4** (34 mg, 0.060 mmol) in THF (5 ml) and PMe_3 (25 μl, 0.246 mmol) was added *via* syringe. The reaction mixture was stirred for 30 min, resulting in the precipitation of an orange solid, and the solvent was removed under vacuum. In the glovebox, the residue was washed with THF, dissolved in CH_3CN, and filtered through a plug of celite. Crystallization of the residue by diffusion of C_6H_6 into a CH_3CN solution afforded air-sensitive **17** with CH_3CN (1:1) (37 mg, 90%): orange crystals, m.p. 208–210°C (dec.); ^1H NMR (300 MHz, CD_3CN) δ 5.61 ("t", $J = 2.3$ Hz, 2 H), 5.57 (br s, 4 H), 5.15 ("t", $J = 2.3$ Hz, 2 H), 2.42 (s, 3 H), 1.48 ("dd", $J(^{31}P-^1H) = 9.9$ Hz, $J(^{103}Rh-^1H) = 0.9$ Hz, 18 H); ^{13}C NMR (100 MHz, CD_3CN) δ 225.90, 93.03 (m), 92.26, 87.40 (m), 86.48, 86.27, 49.92, 18.88 ("t", $J(^{31}P-^{13}C) = 35.2$ Hz), (quaternary carbon from the fulvalene ring bound to ^{103}Rh and $^{103}Rh-C(O)CH_3$ were not observed); ^{31}P NMR (121.5 MHz, CD_3CN) δ 4.69 (d, $J(^{103}Rh-^{31}P) = 157.2$ Hz); IR (KBr) ν(CO) 1890, 1763, 1639 cm^{-1}; FAB-MS (sulfolane), m/z 694 (M^+). Anal. Calcd. for $C_{21}H_{29}O_4P_2RhW(CH_3CN)$: C, 37.55; H, 4.35, N, 1.90. Found: C, 37.69; H, 4.42; N, 1.55.

4.15. X-Ray diffraction analysis of 17

X-ray quality crystals were grown by diffusion of C_6H_6 vapors into a solution of **17** in CH_3CN. Crystal size $0.10 \times 0.20 \times 0.35$ mm^3, space group $P2_1/n$, a = 15.412(4) Å, b = 9.745(2) Å, c = 18.209(6) Å, α = 90.0°, β = 93.46(2)°, γ = 90.0°, V = 2730.0(22) Å^3, $Z = 4$, μ = 50.4 cm^{-1}, $d_{calcd} = 1.83$ g cm^{-3}, radiation: Mo K_α ($\lambda = 0.70926$ Å), 2θ-range: $3° \leqslant 2\theta \leqslant 45°$, scan mode: ω, scan range in ω: 0.8°, temperature: 193 K, reflections collected: 3971, reflections observed: 2682 [$F^2 > 3\sigma(F^2)$], $R = 0.0277$, $R_w = 0.0303$. Atomic coordinates, thermal parameters, and torsional angles are given in the supplementary material.

4.16. FvRh(PMe$_3$)$_2$Me (18)

A solution of **16** (8 mg, 0.020 mmol) in CD_3CN was placed in an NMR tube and degassed using three freeze–pump–thaw cycles. An excess (> 8 equivalents) of PMe_3 was condensed into the tube which was then sealed under vacuum. The sample was allowed to sit overnight at room temperature, the color of the solution changing from orange to red. Analysis by NMR spectroscopy indicated the formation of only one new fulvalene product: ^1H NMR (300 MHz, CD_3CN) δ 5.97 (m, 2 H), 5.70 (m, 2 H), 5.14 (m, 2 H), 4.93 (m, 2 H), 1.24 ("dd", $J(^{31}P-^1H) = 10.5$ Hz, $J(^{103}Rh-^1H) = 0.7$ Hz, 18 H), 0.19 (dt, $J(^{31}P-^1H) = 6.2$ Hz, $J(^{103}Rh-^1H) = 2.4$ Hz, 3 H); ^{31}P NMR (121.5 MHz, CD_3CN) δ 2.48 (d, $J(^{103}Rh-^{31}P) = 150.5$ Hz).

4.17. FvRh(PMe$_3$)$_2$C(O)Me (19)

A solution of **17** (8 mg, 0.019 mmol) in CD_3CN was placed in an NMR tube and degassed using three freeze–pump–thaw cycles. An excess (> 8 equivalents) of PMe_3 was condensed into the tube which was sealed under vacuum. The sample was allowed to sit overnight at room temperature, the color of the solution changing from orange to red. Analysis by NMR spectroscopy indicated the formation of only one new fulvalene product: ^1H NMR (300 MHz, CD_3CN) δ 6.09 (m, 2 H), 5.82 (m, 2 H), 5.52 (m, 2 H), 5.06 (m, 2 H), 2.30 (s, 3 H), 1.26 ("dd", $J(^{31}P-^1H) = 10.8$ Hz, $J(^{103}Rh-^1H)$ 0.8 Hz, 18 H); ^{31}P NMR (121.5 MHz, CD_3CN) δ1.69 (d, $J(^{103}Rh-^{31}P) = 164.0$ Hz).

4.18. Fv[Mo(CO)$_3$][Rh(PMe$_3$)$_2$C(O)CH$_3$] (20)

A Schlenk flask was charged with a deoxygenated solution of **4** (66 mg, 0.116 mmol) in CH_3CN (10 ml), followed by the addition of PMe_3 (0.480 ml, 4.72 mmol) *via* syringe. The reaction mixture was stirred for 26 h and the solvent removed under vacuum. In the glovebox, the residue was dissolved in THF (20 ml) and filtered through a plug of celite to obtain a deep red solution of **19** admixed with *fac*-$W(CO)_3(PMe_3)_3$. A solution of $Mo(CO)_3(EtCN)_3$ (39 mg, 0.113 mmol) in THF (2 ml) was added and the reaction mixture stirred 24 h resulting in an orange precipitate. The solvent was removed under vacuum. In the glovebox, the residue was washed with THF, dissolved in CH_3CN, and filtered through a plug of celite. The solvent was removed under vacuum and the residue recrystallized by diffusion of C_6H_6 into a CH_3CN solution to afford air-sensitive **20** (9 mg, 13%): orange crystals, m.p. 215–217°C (dec.); ^1H NMR (300 MHz, CD_3CN) δ 5.64 ("t", $J = 2.3$ Hz, 2 H), 5.56 (br m, 4 H), 5.15 ("t", $J = 2.3$ Hz, 2 H), 2.41 (s, 3 H), 1.47 ("dd", $J(^{31}P-^1H) = 9.9$ Hz, $J(^{103}Rh-^1H) = 0.7$ Hz, 18 H); ^{13}C NMR (100 MHz, CD_3CN) δ 235.22, 94.08, 92.91 (br), 88.64, 88.60, 86.95

(br), 50.10, 18.88 ("t", $J(^{31}P-^{13}C) = 34.7$ Hz), (quaternary carbons attached to ^{103}Rh were not observed); ^{31}P NMR (121.5 MHz, CD_3CN) δ 4.77 (d, $J(^{103}Rh-^{31}P) = 157.2$ Hz); IR (KBr) ν(CO) 1892, 1773, 1636 cm^{-1}; FAB-MS (sulfolane), m/z 608 (M^+), 427 ($M^+-Mo(CO)_3$).

5. Supplementary material available

X-ray data for compounds **4** and **17** (67 pages) have been deposited with the Cambridge Crystallographic Data Centre, Cambridge, UK.

Acknowledgments

This work was supported by the Director, Office of Energy Research, Office of Basic Energy Sciences, Chemical Sciences Division of the US Department of Energy (DE-AC03-76SF00098). We thank S. Laursen and Professor G.C. Pimentel for the help with the matrix experiment. Furthermore we thank the DAAD for a NATO fellowship (J.B.)

References and notes

1 P.A. McGovern and K.P.C. Vollhardt, *Synlett*, (1990) 493 and references cited therein.
2 R. Boese, M.A. Huffman and K.P.C. Vollhardt, *Angew. Chem., Int. Ed. Engl., 30* (1991) 1463.
3 M.-H. Delville-Desbois, D.S. Brown, K.P.C. Vollhardt and D. Astruc, *J. Chem. Soc., Chem. Commun.*, (1991) 1355.
4 P. Hudeczek and F.H. Köhler, *Organometallics, 11* (1992) 1773 and references cited therein.
5 A.P. Kahn, D.A. Newman, K.P.C. Vollhardt, *Synlett*, (1990) 141.
6 (a) M.D. Rausch, T.E. Gismondi, H.G. Alt and J.A. Schwärtzle, *Z. Naturforsch., Teil B, 32* (1977) 998; (b) T.E. Gismondi and M.D. Rausch, *J. Organomet. Chem., 284* (1985) 59.
7 (a) R.G. Severson and A. Wojcicki, *J. Organomet. Chem., 157* (1978) 173;
(b) D.R. Tyler, *Inorg. Chem., 20* (1981) 2257.
8 H.G. Alt, *Angew. Chem., Int. Ed. Engl., 23* (1984) 766.
9 (a) M. Cheong and F. Basolo, *Organometallics, 7* (1988) 2041; (b) F. Basolo, *Inorg. Chim. Acta, 100* (1985) 33; (c) H.G. Schuster-Woldan and F. Basolo, *J. Am. Chem. Soc., 88* (1966) 1657.
10 A.J. Rest, I. Whitwell, W.A.G. Graham, J.K. Hoyano and A.D. McMaster, *J. Chem. Soc., Dalton Trans.*, (1987) 1181.
11 S.T. Belt, F.-W. Grevels, W.E. Klotzbücher, A. McCamley and R.N. Perutz, *J. Am. Chem. Soc., 111* (1989) 8373.
12 R.H. Crabtree, *Chem. Rev., 85* (1985) 245 and references cited therein.
13 J.S. Drage, M. Tilset, K.P.C. Vollhardt and T.W. Weidman, *Organometallics, 3* (1984) 812.
14 T.E. Bitterwolf and A.L. Rheingold, *Organometallics, 10* (1991) 3856.
15 M.J. Krause and R.G. Bergman, *Organometallics, 5* (1986) 2097.
16 A.J. Hart-Davis and W.A.G. Graham, *Inorg. Chem., 10* (1971) 1653.
17 The longest W–Rh separation uncovered by a search of the Cambridge Crystallographic Database was 2.760(1) Å: (a) M. Chetcuti, M. Green, J.A.K. Howard, S.J. Porter, F.G.A. Stone, A.A. Wilson and P. Woodward, *J. Chem. Soc., Chem. Commun.*, (1980) 1057; (b) M. Green, J.C. Jeffery, S.J. Porter, H. Razay and F.G.A. Stone, *J. Chem. Soc., Dalton Trans.*, (1982) 2475.
18 J.S. Drage and K.P.C. Vollhardt, *Organometallics, 5* (1986) 280.
19 R. Moulton, T.W. Weidman, K.P.C. Vollhardt and A.J. Bard, *Inorg. Chem., 25* (1986) 1846.
20 (a) K.W. Barnett, D.L. Beach, S.P. Gaydos and T.G. Pollmann, *J. Organomet. Chem., 69* (1974) 121;
(b) A. Wojcicki, *Adv. Organomet. Chem., 11* (1973) 87;
(c) K.W. Barnett and P.M. Treichel, *Inorg. Chem., 6* (1967) 294.
21 R. Cramer and L.P. Seiwell, *J. Organomet. Chem., 92* (1975) 245.
22 (a) S.L. Laursen and G.C. Pimentel, *J. Phys. Chem., 93* (1989) 2328;
(b) H.E. Cartland and G.C. Pimentel, *J. Phys. Chem., 90* (1989) 1822.
23 (a) G. Erker and F. Rosenfeldt, *J. Organomet. Chem., 188* (1980) C1; (b) G. Erker and F. Rosenfeldt, *Angew. Chem., Int. Ed. Engl., 17* (1978) 605; (c) G. Fachinetti, G. Fochi and C. Floriani, *J. Chem. Soc., Dalton Trans.*, (1977) 1946.
24 J.P. Collman, L.S. Hegedus, J.R. Norton and R.G. Finke, in *Principles and Applications of Organotransition Metal Chemistry*, University Science Books, Mill Valley, 1987, Chapters 6, 12 and references cited therein.
25 S.M. Baxter, G.S. Ferguson and P.T. Wolczanski, *J. Am. Chem. Soc., 110* (1988) 4231 and references cited therein.
26 G.S. Ferguson, P.T. Wolczanski, L. Párkányi and M.C. Zonnevylle, *Organometallics, 7* (1988) 1967 and references cited therein.
27 M. Tilset and K.P.C. Vollhardt, *Organometallics, 4* (1985) 2230.
28 M.Y. Darensbourg, P. Jimenez, J.R. Sackett, J.M. Hanckel and R.L. Kump, *J. Am. Chem. Soc., 104* (1982) 1521.
29 T.W. Weidman, *Ph.D. Thesis*, University of California, Berkeley, 1987.
30 R. Boese, W.B. Tolman and K.P.C. Vollhardt, *Organometallics, 5* (1986) 582.
31 W.B. Tolman, *Ph.D. Thesis*, University of California, Berkeley, 1988.
32 M.A. Huffman, *Ph.D. Thesis*, University of California, Berkeley, 1988.
33 R. Mathieu, M. Lenzi and R. Poilblanc, *Inorg. Chem., 9* (1970) 2030.
34 U. Behrens and F. Edelmann, *J. Organomet. Chem., 263* (1984) 179.
35 M.A. Huffman, D.A. Newman, M. Tilset, W.B. Tolman and K.P.C. Vollhardt, *Organometallics, 5* (1986) 1926.